A photoactive nickel complex provides evidence for a general Ni(I)/Ni(III) paradigm in cross-coupling catalysis

Lucia Anghileri[1,2,3], Haralds Baunis[1,2,†], Aleksander R. Bena[1,2,†], Christos Giannoudis[1,2,†], John H. Burke[4], Susanne Reischauer[2], Christoph Merschjann[5], Rachel F. Wallik[4], Gianluca Simionato[6], Sergey Kovalenko[7], Luca Dell'Amico[6], Renske M. van der Veen[4,5] and Bartholomäus Pieber[1,2*]

[1]Institute of Science and Technology Austria (ISTA), Am Campus 1, 3400 Klosterneuburg, Austria

[2]Department of Biomolecular Systems, Max-Planck-Institute of Colloids and Interfaces (MPICI), Am Mühlenberg 1, 14476 Potsdam, Germany

[3]Department of Chemistry and Biochemistry, Freie Universität Berlin; Arnimallee 22, 14195 Berlin, Germany

[4]Department of Chemistry, University of Illinois Urbana−Champaign; Urbana, Illinois 61801, United States

[5]Helmholtz Zentrum Berlin für Materialien und Energie GmbH; Hahn-Meitner-Platz 1, 14109 Berlin, Germany

[6]Department of Chemical Sciences, University of Padova, Via Francesco Marzolo 1, 35131 Padova, Italy

[7]Department of Chemistry, Humboldt-Universität zu Berlin, Brook-Taylor-Str. 2, 12489 Berlin, Germany

[†]These authors contributed equally to this work

*Corresponding author. Email: bartholomaeus.pieber@ist.ac.at
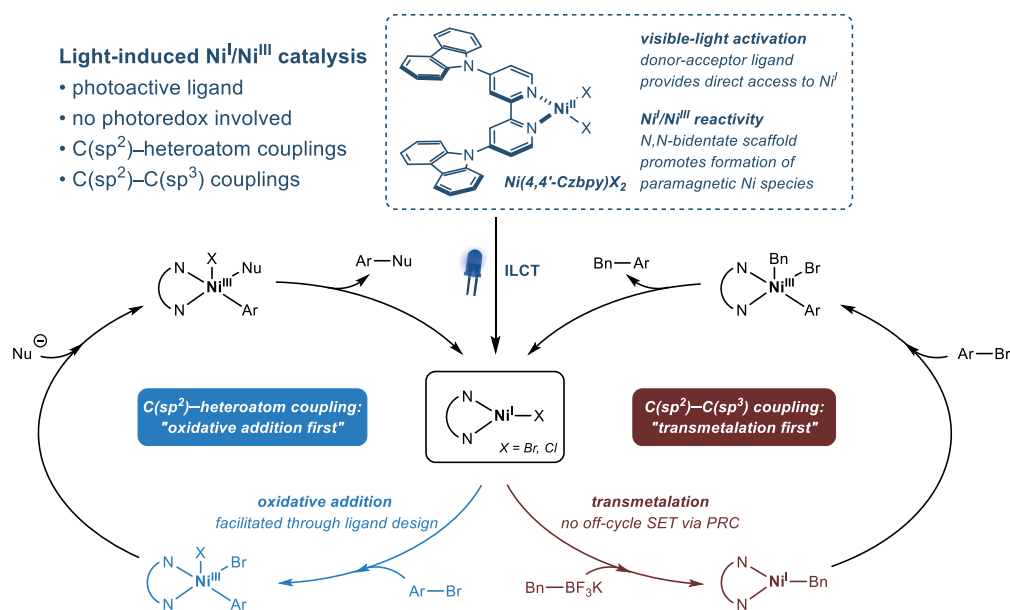
Abstract: Advances in nickel catalysis have significantly broadened the synthetic chemists' toolbox, particularly through methodologies leveraging paramagnetic nickel species via photoredox catalysis or electrochemistry. Nonetheless, the mechanisms of these transformations remain poorly understood. In a pursuit to expand the scope of $C(sp^2)$–heteroatom couplings by modulating the electronic properties of donor-acceptor ligands, we identified a photoactive nickel complex capable of catalyzing $C(sp^2)$–$C(sp^3)$ cross-couplings between aryl halides and benzyltrifluoroborate salts without involving photoredox reactivity. Mechanistic investigations provided compelling evidence that an unprecedented direct transmetalation between a Ni(I) intermediate and the organoboron species serves as pivotal catalytic step. More generally, these findings suggest that photo/electrochemically-mediated nickel-catalyzed $C(sp^2)$–heteroatom and $C(sp^2)$–$C(sp^3)$ bond formations can operate via similar Ni(I)/Ni(III) manifolds.

Introduction

The efficacy of palladium complexes as catalysts for cross-couplings hinges upon fine-tuning the metal's reactivity through stereoelectronic control via tailored ligands. This ability enables the utilization of a wide array of substrates, low catalyst loadings, and mild reaction conditions (Fig. 1, A).[1-4] Over the past decade, the integration of nickel catalysis with single electron transfer (SET) reactivity has emerged as a pivotal platform for alternative and complementary cross-couplings, operating via a fundamentally distinct strategy.[5-10] Instead of modulating the metal's ligand field, these catalytic reactions are orchestrated by manipulating the oxidation state of nickel. This provides several plausible mechanisms that are actively studied and debated. For example, the originally proposed mechanisms of various $C(sp^2)$–heteroatom cross-couplings were recently revised by showing that these reactions proceed through a "dark" Ni^I/Ni^{III} cycle initiated by single electron reduction of a Ni^{II} pre-catalyst (**I**) employing photoredox catalysis (PRC),[11-14] cathodic reduction,[15] or zinc (Fig. 1, B).[16] The mechanism of $C(sp^2)$–$C(sp^3)$ cross-couplings between aryl halides and radical precursors, such as alkyl trifluoroborates, is arguably more complex and was proposed to require several SET events facilitated by PRC[7, 17] or electrochemistry.[18] In these scenarios, single electron reductions are assumed to produce a catalytically active Ni^0 species (**V**) capable of trapping an alkyl radical, which is generated through an off-cycle single electron oxidation of the nucleophile (single electron transmetalation). The resulting Ni^I intermediate (**VI**) undergoes oxidative addition (OA) with the aryl halide, followed by reductive elimination (RE) to afford the desired product. A single electron reduction of the resulting Ni^I species closes the nickel cycle.

Typically, these $C(sp^2)$–heteroatom and $C(sp^2)$–$C(sp^3)$ cross-coupling protocols employ Ni^{II} salts in conjunction with 4,4′-di-*tert*-butyl-2,2′-bipyridine (dtbbpy) as a privileged ligand. The primary role of the *N,N*-bidentate motif is to promote the formation of the key paramagnetic nickel species.[19] Notably, recent studies indicated that alterations in ligand structure influence oxidative addition on Ni^I through steric and electronic effects.[20, 21]

Photoactive nickel complexes obviate the need for exogeneous photocatalysts, electrochemical setups, or addition of chemical reductants in $C(sp^2)$–heteroatom cross-couplings that proceed through the Ni^I/Ni^{III} manifold (Fig. 1, C). Seminal studies by Doyle and colleagues have demonstrated that Ni^{II}(dtbbpy) aryl halide complexes produce Ni^I species upon irradiation with light.[22, 23] Direct excitation generates a metal-to-ligand charge transfer (MLCT) state that transitions to a triplet metal-centered d-d state,[24] or a ligand-to-metal charge transfer (LMCT) state,[25, 26] resulting in homolysis of the Ni^{II}–aryl bond. These complexes have been applied as effective catalysts for C–O and C–N cross-couplings using 390 nm irradiation.[27, 28] The Mirica group has shown that a similar activation mechanism triggers Ni^{II}–Cl bond fission in the case of a Ni(pyridinophane)Cl$_2$ complex to promote C–O bond formations using purple LEDs (390 nm).[29] In the same year, we demonstrated that a nickel complex featuring a donor-acceptor (D-A) ligand harnesses lower energy visible-light (440 nm) through an intraligand charge transfer (ILCT) transition.[30] This accessed the Ni^I/Ni^{III} manifold for $C(sp^2)$–heteroatom bond formations between aryl iodides and *S*-, *N*-, and *O*-nucleophiles via excited state properties that solely depend on the electronics and structure of the ligand scaffold. Li and co-workers followed a different strategy towards photoactive ligands by integrating a quinolinium photoredox catalyst[31] into the bipyridine ligand scaffold.[32] In combination with NiCl$_2$ and a 390 nm light source, this photoredox active ligand facilitates several transformations, including $C(sp^2)$–$C(sp^3)$ couplings between aryl halides and alkyl trifluoroborates.
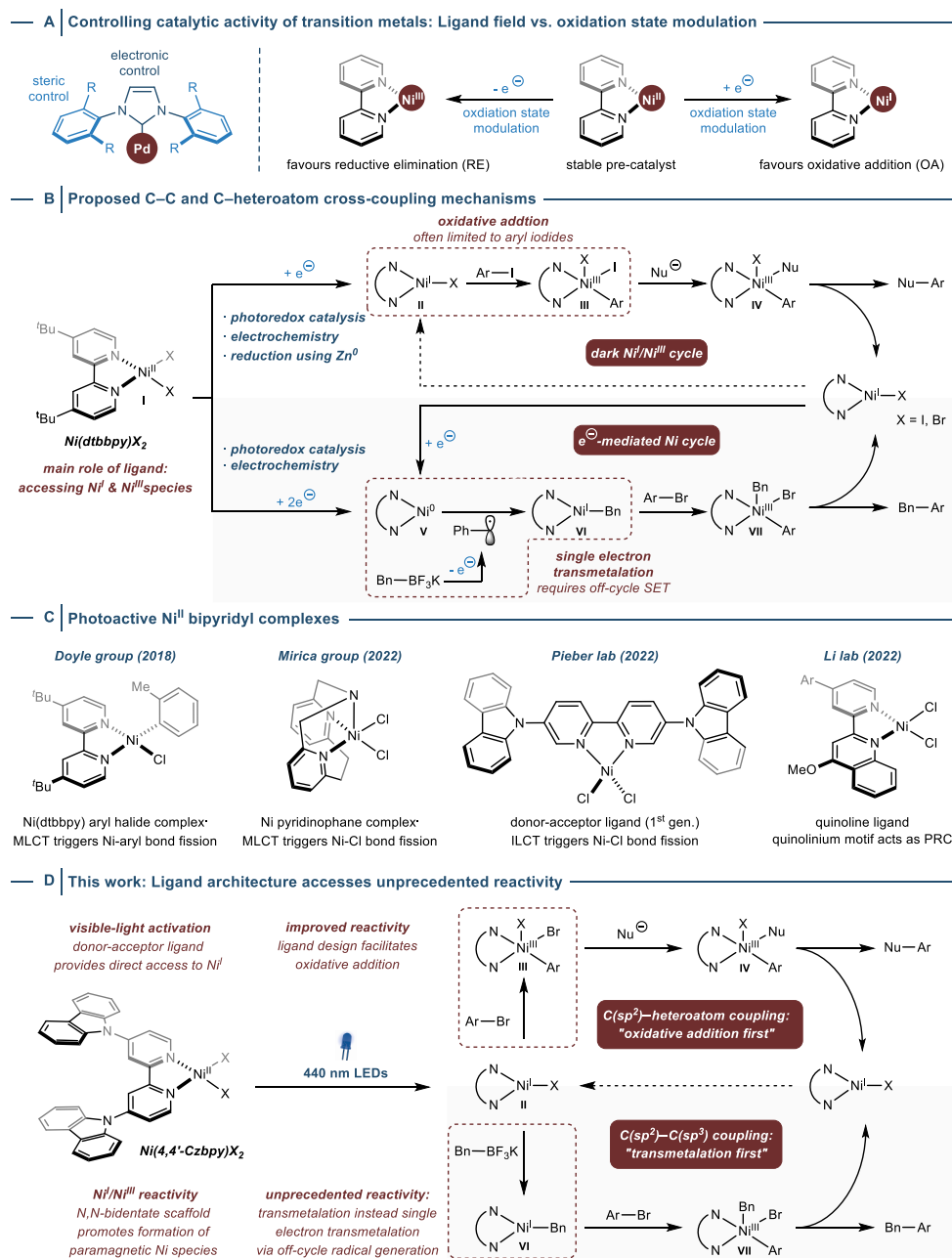
2

Fig 1. Nickel bipyridine complexes as catalysts for cross-couplings. (**A**) Controlling catalytic activity through the ligand field (left) or by modulating the oxidation state through single electron transfer events (right). (**B**) Proposed mechanisms of carbon–heterotaom and carbon-carbon cross-couplings catalyzed by oxidation state modulation of Ni(dtbbpy)X$_2$. (**C**) Photoactive nickel complexes. (**D**) Development of a photactive nickel complex that triggers C–heteroatom and C–C bond formations through Ni^{I}/Ni^{III} manifolds.

We envisioned that rational design of photoactive ligands allows modulating nickel's ligand field to fine-tune catalytic activity. Here, we present our efforts that commenced with the aim to address substrate limitations in C(sp^2)–heteroatom couplings through strategic ligand design and culminated in the serendipitous discovery of an unprecedented paradigm for light-mediated C(sp^2)–C(sp^3) cross-couplings (Fig. 1, D). Our mechanistic investigations provide compelling evidence that photoredox catalytic activity is not required for coupling benzylic trifluoroborate salts with aryl halides. Instead, we show that a photochemically formed Ni^{I} species reacts through a direct transmetalation step with

the organoboron starting material. Our findings provide striking evidence that light-mediated nickel-catalyzed cross-couplings can be generally accessed through a Ni^I/Ni^{III} manifold.

Ligand development

Our research endeavors began with the objective of expanding the applicability of our first-generation donor-acceptor ligand $Ni(5,5'-Czbpy)X_2$ (X = Cl or Br), which was confined to coupling aryl iodides with nucleophiles.[30] We proposed that relocating the electron-donating carbazole units to the 4,4'-position of bipyridine could yield a nickel-ILCT complex with improved catalytic activity, attributed to increased electron density on the crucial Ni^I species facilitating OA.

As a first step to test this hypothesis, we synthesized 4,4'-Czbpy and compared its photophysical properties with its regioisomer 5,5'-Czbpy. The ligands have different static UV/visible absorption spectra (Fig. 2, A, left). While the low-energy ILCT band of 5,5'-Czbpy peaks at 350 nm, the ILCT band of 4,4'-Czbpy is blue-shifted and overlaps with the vibronically resolved carbazole-centered π-π* transition (335 nm).

Pump-probe femtosecond-resolved optical transient absorption (OTA) spectroscopy experiments with excitation at 345 nm showed that both ligands form a long-lived state with a life time of >2 ns and similar transient spectra (Fig. 2, A, left). Density functional theory (DFT) calculations confirm that this state belongs to the lowest triplet (T1) state of mixed ^{3}ILCT/bpy 3(π-π*) character (Fig S30-S34) [33]. Both ligands exhibit a red-shift of the ILCT band upon NiX_2 complexation with an absorption onset in the visible region of the electromagnetic spectrum (Fig S18). When pumped at >400 nm, the complexes show similar transient spectra to the ligands (Fig S16), but with dramatically reduced lifetimes of ~20 ps (Fig 2, A, right). This confirms that the lowest triplet state of both ligands is quenched by NiX_2, which likely occurs by a decay into an optically dark metal-centered d-d state manifold.[30] These d-d states have anti-bonding character along the nickel halide bonds, signifying their propensity for Ni^{II}–halide bond homolysis and the formation of catalytically active Ni^I species.[22, 29, 30] Overall, these results show that nickel complexes of both ligands obey similar excited-state dynamics, but the difference in spectral band positions clearly indicate that the electronic structure is modulated by 4,4'- vs 5,5'-carbazole functionalization of bpy, which ultimately impacts the electronic structure of the Ni center (*vide infra*).

Ligand impacts oxidative addition

The proposed fine-tuning of Ni^I reactivity towards OA through electronic control via the ligand field was ultimately demonstrated in a model $C(sp^2)$–heteroatom cross-coupling (Fig. 2, B). Using 440 nm LEDs, 4,4'-Czbpy served as an efficient ligand for nickel to catalyze the coupling of sodium *p*-toluenesulfinate (**1**) with 4-bromobenzotrifluoride (**2**) (see Table S1-S2 for details). The catalyst loading could be even reduced from 5 to 1 mol% resulting on similar cross-coupling yield. In contrast, only traces of the desired product were obtained when 5,5'-Czbpy was employed. Both ligands proved ineffective in coupling a more challenging electron-rich aryl bromide (**3**). Mechanistic investigations using cyclic voltammetry (CV) corroborated these findings by linking the electrochemical generation of the transient Ni^I species (E-step, peak **A**) with its chemical consumption (C-step) upon reaction with aryl halides (EC-mechanism) (Fig. 2, C).[20, 34] A decrease in reversibility indicated by a lowering of the intensity of return peak **B**, and the emergence of a new species (**C**) signify effective OA, which enables facile qualitative comparison of the reactivity of different aryl halides and nickel complexes. Use of tetrabutylammonium bromide (TBAB) as supporting electrolyte proved crucial for obtaining

4

interpretable CVs. Consequently, and given that the halide identity of Ni[I] bipyridine species was shown to have no significant effect on OA,[21] CV studies were conducted using ligated NiBr$_2$ instead of NiCl$_2$ salts to avoid the presence of multiple halide species potentially affecting the analysis. The electroanalytical approach was first validated using 4-iodobenzotrifluoride, which confirmed that both ligands generate Ni[I] complexes that undergo facile oxidative addition in case of an aryl iodide (Fig. S39 and S43). In agreement with observations from the model reaction, the CV of electrochemically generated Ni(4,4′-Czbpy)Br in the presence of the electron-poor aryl bromide **2**
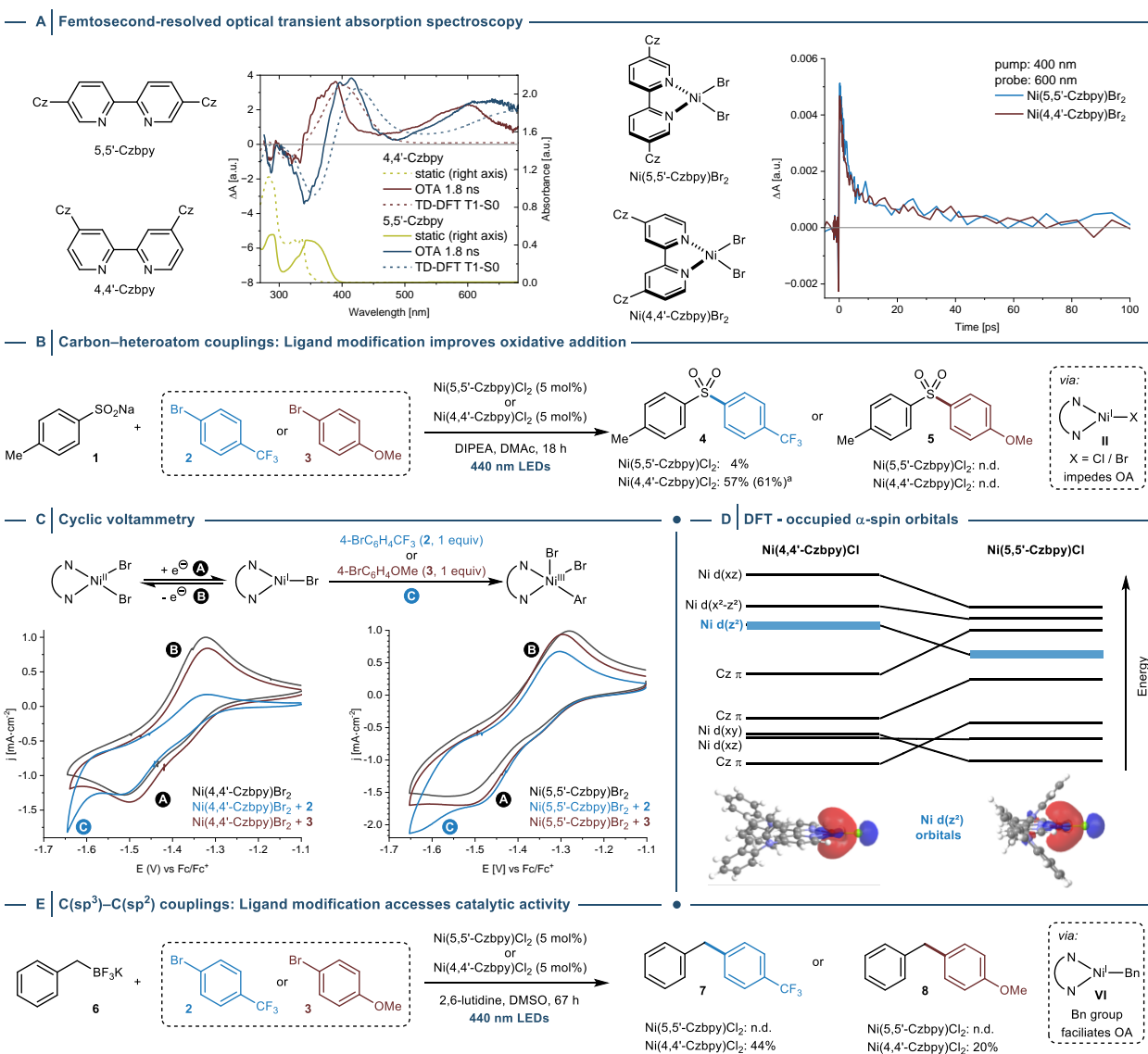

Fig 2. Structural modifications of donor-acceptor ligand impacts catalytic activity in light-mediated nickel-catalyzed cross-couplings. (**A**) Optical transient absorption (OTA) data of ligands (left, 345 nm pump) and NiBr$_2$ complexes (right, 400 nm pump) in DMSO. Left: Transient spectra of ligands at 1.8 ns (left axis) and static absorption spectra (right axis). Transient spectra were simulated by TD-DFT (CAM-B3LYP-GD3/6-311+G(d,p), -0.5 eV shift) by taking the difference of the triplet (T1) and singlet (S0) TD-DFT spectra. Right: kinetic traces of NiBr2 complexes at a probe wavelength of 600 nm, showing a pronounced decrease in excited-state lifetime compared to the free ligands. (**B**) 4,4′-Czbpy outperforms its regioisomer (5,5′-Czbpy) as ligand for light-mediated nickel catalyzed C–S couplings by facilitating OA as evidenced by CV studies (**C**). (**D**) Comparison of DFT orbital energies indicate that the 3d(z^2) orbital of Ni(4,4′-Czbpy)Cl is destabilized and reactive towards OA. CAM-B3LYP-GD3/6-311+G(d,p) (**E**) The modified D-A ligand enables C(sp^2)–C(sp^3) cross-couplings between benzyl trifluoroborates and aryl bromides. [a]Yield in brackets refers to reaction carried out using 1 mol% of Ni(4,4′-Czbpy)Cl$_2$.

revealed a notable loss in reversibility, whereas this effect was significantly less pronounced with 5,5′-Czbpy.[35] The electron-rich aryl bromide **3**, which failed to yield the desired C–S coupling product with both ligands, induced no substantial alterations in the reversibility of the Ni^I/Ni^{II} couples.

DFT calculations were employed to investigate the electronic structure of the reactive Ni^I species. Previous studies established the significance of the $3d(z^2)$ orbital in the OA of aryl halides to Ni^I complexes, with electron-donating substituents enhancing the rate of this reaction by destabilizing Ni orbitals, including the $3d(z^2)$ orbital.[21] The isomeric nature of Ni(4,4′-Czbpy)Cl and Ni(5,5′-Czbpy)Cl allows for a direct comparison of their orbital energies through Kohn-Sham DFT (Fig. 2, D). The substitution pattern of 4,4′-Czbpy results in destabilization of the 3d orbitals of the respective Ni^I–Cl complex compared its regioisomer Ni(5,5′-Czbpy)Cl, leading to a higher energy of the $3d(z^2)$ orbital that is responsible for the observed difference in OA efficacy.

Ligand enables $C(sp^2)$–$C(sp^3)$ couplings

After identifying that strategic modification of a photoactive ILCT ligand expands the scope of $C(sp^2)$–heteroatom couplings, we wondered whether these structural changes impact (photo)catalytic activity of the corresponding nickel complex regarding $C(sp^2)$–$C(sp^3)$ couplings. Previously, we demonstrated that Ni(5,5′-Czbpy)Cl$_2$ has moderate catalytic activity towards the light-mediated coupling between an aryl iodide and an α-silylamine that was proposed to proceed through off-cycle generation of a C–centered radical,[30] but failed entirely to couple organotrifluoroborate **6**, that shares a similar proposed mechanism (Fig. 2, E).[36, 37] Encouragingly, we found that employing 4,4′-Czbpy as a ligand overcomes this limitation: The second-generation ILCT complex facilitated $C(sp^2)$–$C(sp^3)$ bond formation of **6** with both an electron-poor (**2**), and electron-rich aryl bromide (**3**). The difference in aryl halide reactivity when compared to $C(sp^2)$–heteroatom couplings (OA of Ni^I halide into aryl halide), aligns with the mechanistic rational which proposes that the more electron-rich Ni^I benzyl intermediate (**VI**) undergoes oxidative addition.[36, 37]

Careful investigation of all reaction parameters using the coupling between **6** and **2** as model reaction (Table S3-S9), provided optimized conditions that allows quantitative formation of the desired product **7** (Fig. 3). A reaction using the respective aryl chloride resulted in 21% of the coupling product, which shows that this catalytic system is not limited to the use of aryl bromides. Next, the catalytic protocol was evaluated using several aryl bromides and benzyltrifluoroborate salts (Fig. 3). Substrates were selected strategically to enable comparison with the scope of the seminal protocol using dual nickel/photoredox catalysis,[17] which was attempted to study if the two catalytic systems operate through similar or different mechanisms. High levels of versatility and functional group tolerance were observed regarding the aryl bromide partner, and the corresponding coupling products were obtained in good to excellent yield (**7**, **9-25**) (Fig. 3, A). Comparatively, the nature of the benzyltrifluoroborate component affected the yield of the cross-coupling protocol (Fig. 3, B). Electron-rich benzyltrifluoroborates proceeded smoothly to give the respective products in high yields (**26-30**), in contrast, when electron-poor nucleophiles were utilized lower yields were obtained (**31-34**). These results are consistent with the reported data using a catalytic cocktail that includes a nickel source, dtbbpy as ligand and an exogenous photoredox catalyst.[17] Further, the presence of 1,2-diarylethane side-products in all reactions suggested that C–centered radicals are formed from the trifluoroborate salts during catalysis. However, we were surprised to find that the observed limitations

6

of Ni(4,4′-Czbpy)Br$_2$ catalysis included the use of (α-methyl)benzyltrifluoroborate **38** (Fig. 3, C), a substrate that can be smoothly coupled in protocols that apply dual nickel/photoredox catalysis.[17, 36, 38] This subtle difference in the cross-coupling scope suggested that Ni(4,4′-Czbpy)Br$_2$ might trigger cross-couplings through a different mechanism.
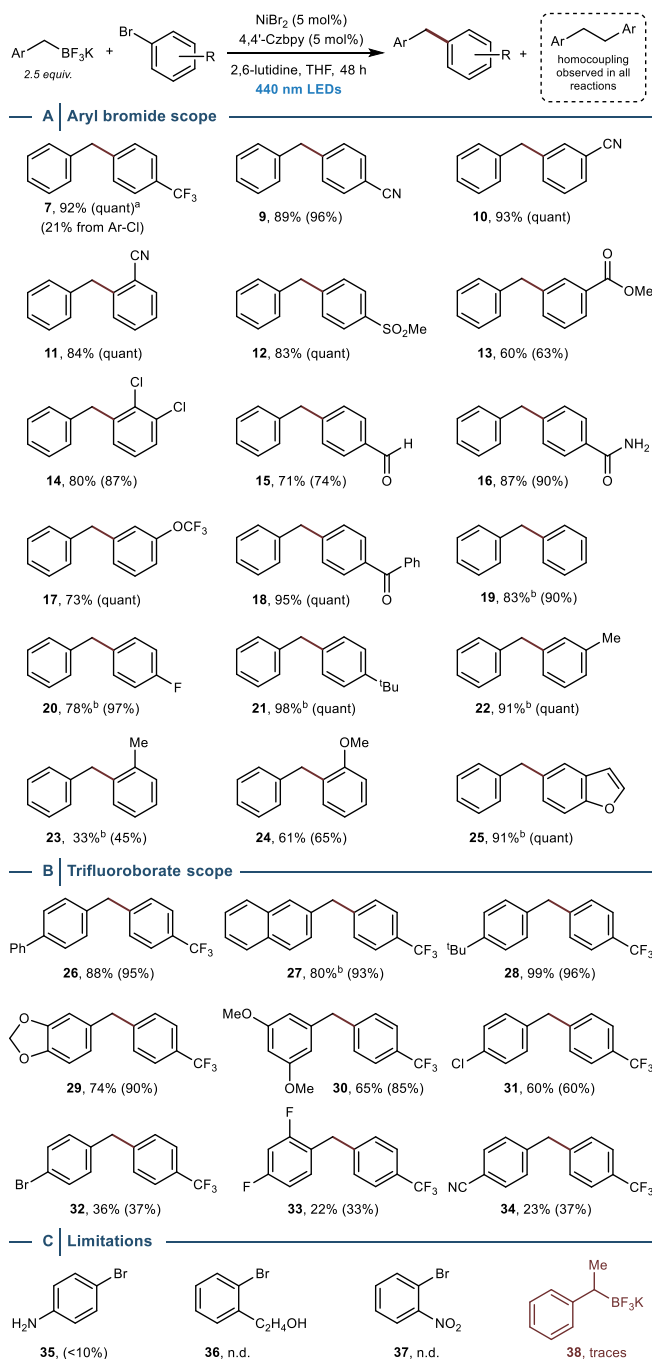

Fig 3. Scope of light-mediated C(sp^2)–C(sp^3) cross-couplings catalyzed by Ni(4,4′-Czbpy)Br$_2$. (**A**) Aryl bromide scope. (**B**) Benzyl trifluoroborate scope. (**C**) Limitations. Isolated yields are reported. [a]NMR yields in brackets were determined by ^{1}H-NMR using 1,3,5-trimethoxybenzene as internal standard. [b]Isolated products contain 6-15% of the unseparable 1,2-diarylethane homocoupling side-product. n.d. = not detected.

Mechanistic studies

Detailed mechanistic investigations were carried out to shed light on the cross-coupling mechanism using the photoactive nickel complex (Fig. 4). In contrast to photoredox catalysts that have sufficiently long excited state lifetimes (<1 ns[39]) resulting in characteristic fluorescence or phosphorescence spectra upon excitation,[40] Ni(4,4′-Czbpy)Br$_2$ does not exhibit pronounced steady-state luminescence when irradiated at wavelengths that are employed for cross-coupling catalysis (>380 nm) (Fig. 4, A, left). This is in agreement with our observations during OTA experiments that showed the excited state ILCT lifetime of Ni(4,4′-Czbpy)Br$_2$ is not sufficient (~20 ps) for a bimolecular SET event between the excited nickel complex and a benzyltrifluoroborate salt when pumped at 400 nm (Fig. 2, A, right). Interestingly, the fluorescence spectra recorded from solutions of the photoactive nickel complex at various excitation wavelengths are qualitatively indistinguishable from those obtained from the measurements employing the free ligand 4,4′-Czbpy (Fig. 4, A, right). Similarly, time-correlated single-photon counting experiments using 340 nm irradiation showed that fluorescence lifetimes of Ni(4,4′-Czbpy)Br$_2$ (14.14 ns) and 4,4′-Czbpy (14.15 ns) are virtually identical (Fig. S14-S15). Together, these observations clearly indicate that the steady-state fluorescence of solutions containing Ni(4,4′-Czbpy)Br$_2$ (1:1) is dominated by unbound ligand (K_{eq}(DMSO) = 5.5·10^4 M^{-1}; K_{eq}(THF) = 7.7·10^5 M^{-1}; see Fig. S7-S11 for details) that does not absorb visible-light.

Emission of the 440 nm LEDs used in synthetic cross-coupling experiment does not overlap with the absorption profile of 4,4′-Czbpy that is responsible for the observed steady-state fluorescence (Fig. S3). However, since Ni(4,4′-Czbpy)Br$_2$ is in equilibrium with unbound ligand in solution, and because 4,4′-Czbpy has an excited state lifetime that meets the requirements for photocatalysis, we performed fluorescence quenching studies at 380 (Fig. 4, B) and 340 nm (Fig. S46) using potassium benzyltrifluoroborate (**6**) in large excess (500 equiv). Both experiments showed that presence of **6** does not impact the emission of Ni(4,4′-Czbpy)Br$_2$ and suggested that the C(sp^2)–C(sp^3) cross-coupling does not proceed via a photoredox catalytic single electron oxidation of **6**.

As a consequence of all results obtained from spectroscopic investigations, we departed from the idea that Ni(4,4′-Czbpy)Br$_2$ triggers C(sp^2)–C(sp^3) bond formations between trifluoroborate salts and aryl halides through a mechanism that involves photocatalytic radical generation followed by reacting with a Ni^0 species (single electron transmetalation). Instead, we hypothesized that generation of Ni^I halide **II** through a light-induced ILCT transition[30] could be followed by a direct transmetalation step with benzylic trifluoroborate salts (Fig. 4, C). This would provide an alternative mechanistic blueprint to access Ni^I alkyl intermediate **VI** that is expected to undergo facile and irreversible oxidative addition of aryl halides.[36] Since such Ni^I alkyl species are prone to decomposition and/or bond homolysis,[41] C–centered radicals that are responsible for homocoupling side-products may be exclusively generated through an undesired pathway.

To test this mechanistic proposal, we conducted a CV experiment using a mixture of Ni(4,4′-Czbpy)Br$_2$ and **6** (Fig. 4, D, red). To our delight, we indeed observed significant changes in the CV compared to a reference experiment using only Ni(4,4′-Czbpy)Br$_2$: A decrease of the return oxidation peak height (**B**) and appearance of a new peak (**D**). The lower potential of **D** compared to **B** is indicative of a more electronegative Ni^I species, such as the proposed transmetalation product Ni(4,4′-Czbpy)Bn (**VI**) (Fig 4, D, right).

8

Grignard reagents are known to undergo transmetalation with L_nNi^I and L_nNi^{II} halides,[41, 42] which allows accessing **VI** via two pathways applying single electron reduction (Fig 4, D, right). This provided the opportunity for a reference CV study using BnMgBr (**39**) and Ni(4,4′-Czbpy)Br$_2$ (Fig. 4, D, light blue). To our delight, this experiment also resulted in appearance of **D**, confirming that this peak is characteristic for Ni^I alkyl species **VI**. With this unambigous evidence for the transmetalation hypothesis in hand, we next performed a CV experiment using Ni(4,4′-Czbpy)Br$_2$ in presence of potassium (α-methyl)benzyltrifluoroborate (**38**) (Fig. 4, D, dark blue). The resulting CV is similar to the reference experiment (only Ni(4,4′-Czbpy)Br$_2$) and does not indicate formation of a transmetalated species. This is in agreement with the observation that **38** is not suitable for light-mediated C(sp^2)–C(sp^3) cross-couplings catalyzed by Ni(4,4′-Czbpy)Br$_2$ (Fig. 3, C). Although it is unclear if the steric demand of the methyl group of **38** is the sole reason for the low reactivity towards

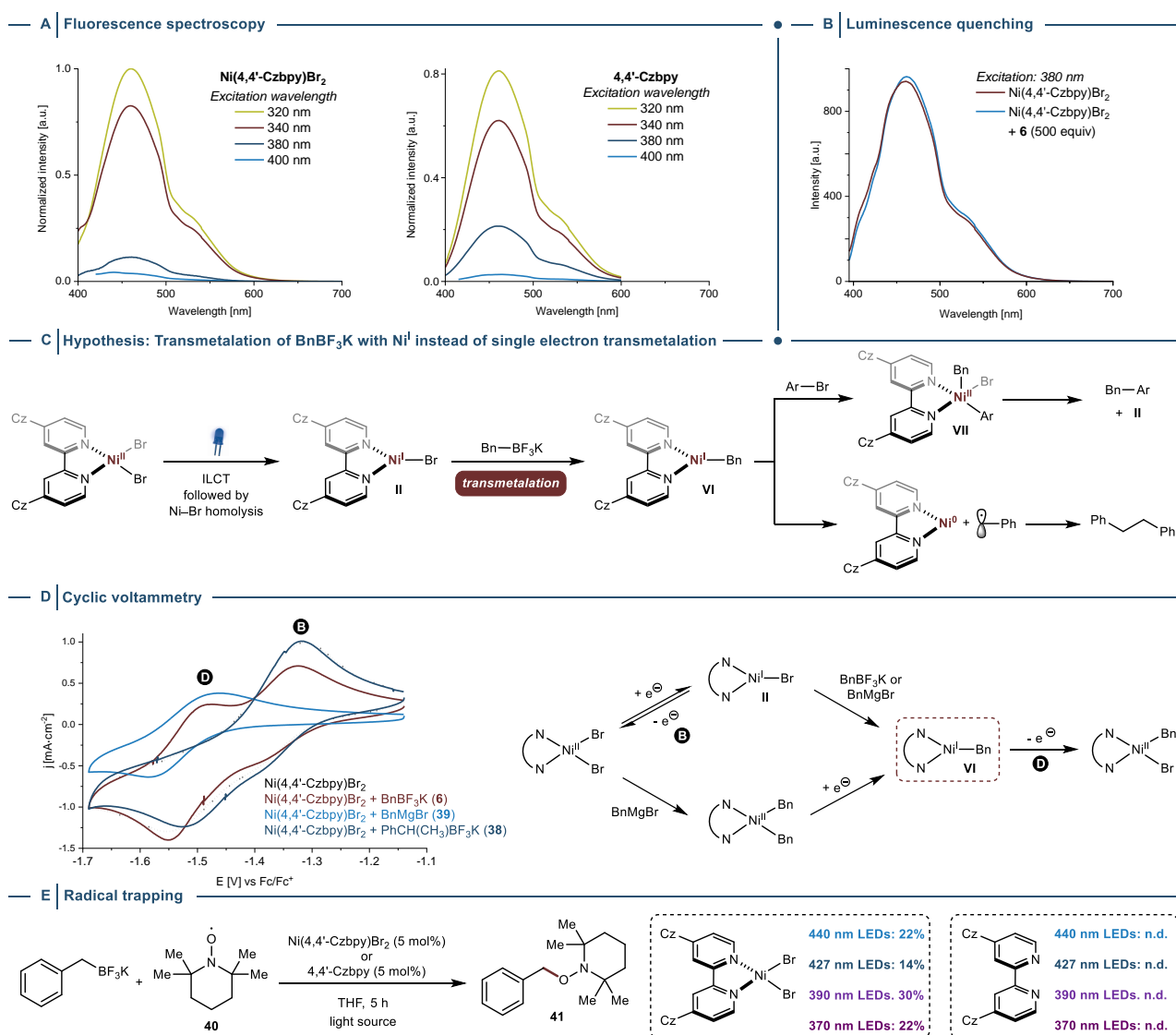**Fig 4. Mechanistic investigations** (**A**). Steady state fluorescence spectroscopy of Ni(4,4′-Czbpy)Br$_2$ and 4,4′-Czbpy are virtually identical and show no significant emission when irradiated >380 nm. (**B**) Luminescence quenching of Ni(4,4′-Czbpy)Br$_2$ is not observed in presence of BnBF$_3$K. (**C**) Proposed mechanism. (**D**) CV experiment shows that transmetalation between a Ni^I halide and BnBF3K is feasible. (**E**) Radical trapping experiments indicate that a C–centered radical is formed upon decomposition of Ni(4,4′-Czbpy)Bn.

9

transmetalation, this result is in line with studies in palladium catalysis that showed that transmetalation rates of secondary alkylboronic acid derivatives appear to be even slower than those of primary analogs.[43] However, our CV experiments demonstrate that this electroanalytical technique is diagnostic for screening the reactivity of nucleophiles towards light-mediated $C(sp^2)$–$C(sp^3)$ cross-couplings catalyzed by Ni(4,4′-Czbpy)Br$_2$. .

Having confirmed that neither Ni(4,4′-Czbpy)Br$_2$, nor 4,4′-Czbpy are effective photoredox catalysts for oxidizing **6**, and that transmetalation between Ni(4,4′-Czbpy)Br (**II**) and primary benzylic trifluoroborates is feasible, we finally carried out a series of trapping experiments to study if the transmetalation product Ni(4,4′-Czbpy)Bn (**VI**) is a source of C-centered radicals (Fig. 4, E). Irradiation of a mixture of Ni(4,4′-Czbpy)Br$_2$, **6** and (2,2,6,6-tetramethylpiperidin-1-yl)oxyl (TEMPO, **40**) using various wavelengths indeed resulted in the desired adduct **41** in moderate yields, whereas no trapping product was detected in the absence of nickel. Together with the above discussed spectroscopic and electroanalytical investigations, these results indicate that **VI** is prone to undergo Ni–benzyl bond homolysis, which supports our mechanistic proposal and provides an explanation for the observations of homocoupling side-products in the $C(sp^2)$–$C(sp^3)$ cross-coupling experiments.

Conclusion

In summary, we demonstrated that the catalytic activity of photoactive nickel complexes can be adjusted through electronic modifications of ligands. Strategic tuning of nickel's electron density through the ligand field enabled expansion of the $C(sp^2)$–S cross-coupling scope to a previously unreactive aryl bromide by facilitating oxidative addition. More importantly, the same ligand modification accessed light-mediated $C(sp^2)$–$C(sp^3)$ cross-couplings between aryl halides and benzyltrifluoroborate salts without exogeneous photoredox catalysts. Mechanistic investigations unveiled that transmetalation between a photochemically generated Ni^I species and a nucleophile is the pivotal catalytic step, as opposed to the generation of a C–centered radical followed by a single electron transmetalation. These findings show that photo/electrochemically-mediated nickel-catalyzed $C(sp^2)$–heteroatom and $C(sp^2)$–$C(sp^3)$ cross-couplings can be generally harnessed via Ni^I/Ni^{III} cycles.

Competing interests: Authors declare that they have no competing interests.

References and Notes

(1) Johansson Seechurn, C. C.; Kitching, M. O.; Colacot, T. J.; Snieckus, V. Palladium-catalyzed cross-coupling: a historical contextual perspective to the 2010 Nobel Prize. *Angew. Chem. Int. Ed.* **2012**, *51*, 5062-5085

(2) Roy, D.; Uozumi, Y. Recent Advances in Palladium-Catalyzed Cross-Coupling Reactions at ppm to ppb Molar Catalyst Loadings. *Adv. Synth. Catal.* **2018**, *360*, 602-625

(3) Littke, A. F.; Fu, G. C. Palladium-Catalyzed Coupling Reactions of Aryl Chlorides. *Angew. Chem. Int. Ed.* **2002**, *41*, 4176-4211

(4) Ruiz-Castillo, P.; Buchwald, S. L. Applications of Palladium-Catalyzed C–N Cross-Coupling Reactions. *Chem. Rev.* **2016**, *116*, 12564-12649

(5) Skubi, K. L.; Blum, T. R.; Yoon, T. P. Dual Catalysis Strategies in Photochemical Synthesis. *Chem. Rev.* **2016**, *116*, 10035-10074

(6) Chan, A. Y.; Perry, I. B.; Bissonnette, N. B.; Buksh, B. F.; Edwards, G. A.; Frye, L. I.; Garry, O. L.; Lavagnino, M. N.; Li, B. X.; Liang, Y.; et al. Metallaphotoredox: The Merger of Photoredox and Transition Metal Catalysis. *Chem. Rev.* **2022**, *122*, 1485-1542

(7) Milligan, J. A.; Phelan, J. P.; Badir, S. O.; Molander, G. A. Alkyl Carbon-Carbon Bond Formation by Nickel/Photoredox Cross-Coupling. *Angew. Chem. Int. Ed.* **2019**, *58*, 6152-6163

(8) Zhu, C.; Yue, H.; Jia, J.; Rueping, M. Nickel-Catalyzed C-Heteroatom Cross-Coupling Reactions under Mild Conditions via Facilitated Reductive Elimination. *Angew. Chem. Int. Ed.* **2021**, *60*, 17810-17831

(9) Palkowitz, M. D.; Emmanuel, M. A.; Oderinde, M. S. A Paradigm Shift in Catalysis: Electro- and Photomediated Nickel-Catalyzed Cross-Coupling Reactions. *Acc. Chem. Res.* **2023**, *56*, 2851-2865

(10) Tay, N. E. S.; Lehnherr, D.; Rovis, T. Photons or Electrons? A Critical Comparison of Electrochemistry and Photoredox Catalysis for Organic Synthesis. *Chem. Rev.* **2022**, *122*, 2487-2649

(11) Ghosh, I.; Shlapakov, N.; Karl, T. A.; Düker, J.; Nikitin, M.; Burykina, J. V.; Ananikov, V. P.; König, B. General cross-coupling reactions with adaptive dynamic homogeneous catalysis. *Nature* **2023**, *619*, 87-93

(12) Till, N. A.; Tian, L.; Dong, Z.; Scholes, G. D.; MacMillan, D. W. C. Mechanistic Analysis of Metallaphotoredox C-N Coupling: Photocatalysis Initiates and Perpetuates Ni(I)/Ni(III) Coupling Activity. *J. Am. Chem. Soc.* **2020**, *142*, 15830-15841

(13) Sun, R.; Qin, Y.; Ruccolo, S.; Schnedermann, C.; Costentin, C.; Daniel, G. N. Elucidation of a Redox-Mediated Reaction Cycle for Nickel-Catalyzed Cross Coupling. *J. Am. Chem. Soc.* **2019**, *141*, 89-93

(14) Till, N. A.; Oh, S.; MacMillan, D. W. C.; Bird, M. J. The Application of Pulse Radiolysis to the Study of Ni(I) Intermediates in Ni-Catalyzed Cross-Coupling Reactions. *J. Am. Chem. Soc.* **2021**, *143*, 9332-9337

(15) Kawamata, Y.; Vantourout, J. C.; Hickey, D. P.; Bai, P.; Chen, L.; Hou, Q.; Qiao, W.; Barman, K.; Edwards, M. A.; Garrido-Castro, A. F.; et al. Electrochemically Driven, Ni-Catalyzed Aryl Amination: Scope, Mechanism, and Applications. *J. Am. Chem. Soc.* **2019**, *141*, 6392-6402

(16) Sun, R.; Qin, Y.; Nocera, D. G. General Paradigm in Photoredox Nickel-Catalyzed Cross-Coupling Allows for Light-Free Access to Reactivity. *Angew. Chem. Int. Ed.* **2020**, *59*, 9527-9533

(17) Tellis, J. C.; Kelly, C. B.; Primer, D. N.; Jouffroy, M.; Patel, N. R.; Molander, G. A. Single-Electron Transmetalation via Photoredox/Nickel Dual Catalysis: Unlocking a New Paradigm for sp3–sp2 Cross-Coupling. *Acc. Chem. Res.* **2016**, *49*, 1429-1439

(18) Luo, J.; Hu, B.; Wu, W.; Hu, M.; Liu, T. L. Nickel-Catalyzed Electrochemical C(sp3)−C(sp2) Cross-Coupling Reactions of Benzyl Trifluoroborate and Organic Halides. *Angew. Chem. Int. Ed.* **2021**, *60*, 6107-6116

(19) Diccianni, J. B.; Diao, T. Mechanisms of Nickel-Catalyzed Cross-Coupling Reactions. *Trends Chem.* **2019**, *1*, 830-844

(20) Tang, T.; Hazra, A.; Min, D. S.; Williams, W. L.; Jones, E.; Doyle, A. G.; Sigman, M. S. Interrogating the Mechanistic Features of Ni(I)-Mediated Aryl Iodide Oxidative Addition Using Electroanalytical and Statistical Modeling Techniques. *J. Am. Chem. Soc.* **2023**, *145*, 8689-8699

(21) Cagan, D. A.; Bím, D.; McNicholas, B. J.; Kazmierczak, N. P.; Oyala, P. H.; Hadt, R. G. Photogenerated Ni(I)–Bipyridine Halide Complexes: Structure–Function Relationships for Competitive C(sp2)–Cl Oxidative Addition and Dimerization Reactivity Pathways. *Inorg. Chem.* **2023**, *62*, 9538-9551

(22) Ting, S. I.; Garakyaraghi, S.; Taliaferro, C. M.; Shields, B. J.; Scholes, G. D.; Castellano, F. N.; Doyle, A. G. 3d-d Excited States of Ni(II) Complexes Relevant to Photoredox Catalysis: Spectroscopic Identification and Mechanistic Implications. *J. Am. Chem. Soc.* **2020**, *142*, 5800-5810

(23) Shields, B. J.; Kudisch, B.; Scholes, G. D.; Doyle, A. G. Long-Lived Charge-Transfer States of Nickel(II) Aryl Halide Complexes Facilitate Bimolecular Photoinduced Electron Transfer. *J. Am. Chem. Soc.* **2018**, *140*, 3035-3039

(24) Ting, S. I.; Garakyaraghi, S.; Taliaferro, C. M.; Shields, B. J.; Scholes, G. D.; Castellano, F. N.; Doyle, A. G. (3)d-d Excited States of Ni(II) Complexes Relevant to Photoredox Catalysis: Spectroscopic Identification and Mechanistic Implications. *J. Am. Chem. Soc.* **2020**, *142*, 5800-5810

(25) Cagan, D. A.; Bím, D.; Silva, B.; Kazmierczak, N. P.; McNicholas, B. J.; Hadt, R. G. Elucidating the Mechanism of Excited-State Bond Homolysis in Nickel–Bipyridine Photoredox Catalysts. *J. Am. Chem. Soc.* **2022**, *144*, 6516-6531

(26) Cagan, D. A.; Stroscio, G. D.; Cusumano, A. Q.; Hadt, R. G. Multireference Description of Nickel–Aryl Homolytic Bond Dissociation Processes in Photoredox Catalysis. *J. Phys. Chem. A* **2020**, *124*, 9915-9922

(27) Li, G.; Yang, L.; Liu, J. J.; Zhang, W.; Cao, R.; Wang, C.; Zhang, Z.; Xiao, J.; Xue, D. Light-Promoted C-N Coupling of Aryl Halides with Nitroarenes. *Angew. Chem. Int. Ed.* **2021**, *60*, 5230-5234

(28) Yang, L.; Lu, H. H.; Lai, C. H.; Li, G.; Zhang, W.; Cao, R.; Liu, F.; Wang, C.; Xiao, J.; Xue, D. Light-Promoted Nickel Catalysis: Etherification of Aryl Electrophiles with Alcohols Catalyzed by a Ni(II) -Aryl Complex. *Angew. Chem. Int. Ed.* **2020**, *59*, 12714-12719

(29) Na, H.; Mirica, L. M. Deciphering the mechanism of the Ni-photocatalyzed C–O cross-coupling reaction using a tridentate pyridinophane ligand. *Nat. Commun.* **2022**, *13*, 1313

(30) Cavedon, C.; Gisbertz, S.; Reischauer, S.; Vogl, S.; Sperlich, E.; Burke, J. H.; Wallick, R. F.; Schrottke, S.; Hsu, W.-H.; Anghileri, L.; et al. Intraligand Charge Transfer Enables Visible-Light-Mediated Nickel-Catalyzed Cross-Coupling Reactions. *Angew. Chem. Int. Ed.* **2022**, *61*, e202211433

12

(31) Li, J.; Huang, C.-Y.; Han, J.-T.; Li, C.-J. Development of a Quinolinium/Cobaloxime Dual Photocatalytic System for Oxidative C–C Cross-Couplings via H2 Release. *ACS Catal.* **2021**, *11*, 14148-14158

(32) Li, J.; Huang, C.-Y.; Li, C.-J. Two-in-one metallaphotoredox cross-couplings enabled by a photoactive ligand. *Chem* **2022**, *8*, 2419-2431

(33) The transient spectrum of 5,5'-Czbpy was reproduced by taking the difference of the T1 spectrum with the lowest singlet (S0) spectrum. This procedure yields agreement for 4,4'-Czbpy in the 280-450 nm region, but underestimates the strength of the excited-state absorption at 600 nm. Calculations with the B3LYP, instead of CAM-B3LYP, functional showed improved agreement (see SI for details).

(34) Rafiee, M.; Abrams, D. J.; Cardinale, L.; Goss, Z.; Romero-Arenas, A.; Stahl, S. S. Cyclic voltammetry and chronoamperometry: mechanistic tools for organic electrosynthesis. *Chem. Soc. Rev.* **2024**, *53*, 566-585

(35) It is noteworthy that substituents adjacent to the nitrogen atoms of bipyridine, which were previously required to stabilize NiI species to achieve CVs with electrochemical reversibility of the NiI/NiII couple,(Ref. 20) are not necessary in case of D-A ligands.

(36) Gutierrez, O.; Tellis, J. C.; Primer, D. N.; Molander, G. A.; Kozlowski, M. C. Nickel-Catalyzed Cross-Coupling of Photoredox-Generated Radicals: Uncovering a General Manifold for Stereoconvergence in Nickel-Catalyzed Cross-Couplings. *J. Am. Chem. Soc.* **2015**, *137*, 4896-4899

(37) Yuan, M.; Song, Z.; Badir, S. O.; Molander, G. A.; Gutierrez, O. On the Nature of C(sp3)–C(sp2) Bond Formation in Nickel-Catalyzed Tertiary Radical Cross-Couplings: A Case Study of Ni/Photoredox Catalytic Cross-Coupling of Alkyl Radicals and Aryl Halides. *J. Am. Chem. Soc.* **2020**, *142*, 7225-7234

(38) Khamrai, J.; Ghosh, I.; Savateev, A.; Antonietti, M.; König, B. Photo-Ni-Dual-Catalytic C(sp2)–C(sp3) Cross-Coupling Reactions with Mesoporous Graphitic Carbon Nitride as a Heterogeneous Organic Semiconductor Photocatalyst. *ACS Catal.* **2020**, *10*, 3526-3532

(39) Romero, N. A.; Nicewicz, D. A. Organic Photoredox Catalysis. *Chem. Rev.* **2016**, *116*, 10075-10166

(40) Buzzetti, L.; Crisenza, G. E. M.; Melchiorre, P. Mechanistic Studies in Photocatalysis. *Angew. Chem. Int. Ed.* **2019**, *58*, 3730-3747

(41) Somerville, R. J.; Odena, C.; Obst, M. F.; Hazari, N.; Hopmann, K. H.; Martin, R. Ni(I)–Alkyl Complexes Bearing Phenanthroline Ligands: Experimental Evidence for CO2 Insertion at Ni(I) Centers. *J. Am. Chem. Soc.* **2020**, *142*, 10936-10941

(42) Griego, L.; Chae, J. B.; Mirica, L. M. A bulky 1,4,7-triazacyclononane and acetonitrile, a Goldilocks system for probing the role of NiIII and NiI centers in cross-coupling catalysis. *Chem* **2024**, *10*, 867-881

(43) Doucet, H. Suzuki–Miyaura Cross-Coupling Reactions of Alkylboronic Acid Derivatives or Alkyltrifluoroborates with Aryl, Alkenyl or Alkyl Halides and Triflates. *Eur. J. Org. Chem.* **2008**, *2008*, 2013-2030